

# SCIENTIFIC REPORTS



OPEN

## Investigation of the hydrophobic and acoustic properties of bio windmill palm materials

Changjie Chen<sup>1,2</sup>, Zhong Wang<sup>1,2</sup>, You Zhang<sup>1</sup>, Ming Bi<sup>1,2</sup>, Kaiwei Nie<sup>1</sup> & Guohe Wang<sup>1,2</sup>

Windmill palm fibers are an abundant lignin-cellulose fiber resource. Single palm fibers can be prepared using an alkali treatment method. However, these fibers have hydrophilic surfaces, and following drying the fibers exhibit serious aggregation. This limits their application as acoustic materials. In this work, both alkali and acetylation treatments were used to modify the characteristics of windmill palm fibers. These treatments caused the surface of the fibers to become hydrophobic and increased the specific area and free vacuum space of the fibers, thus lowering energy loss. Scanning electron microscope observations combined with Fourier-transform infrared spectroscopy showed that the acetylation treatment resulted in the substitution of hydroxyl groups with acetyl groups, and the formation of nanoscale pores (10–50 nm). The results of the moisture-absorption and contact-angle tests showed that the moisture regain value decreased to 3.86%, and the contact angle increased to above 140° after acetylation treatment. The average sound absorption coefficients of the alkalinized and acetylated nonwoven fabrics were 0.31 and 0.36, respectively. The masses of the acetylated samples were 50% those of the windmill palm sheath samples.

With growing global environmental awareness, there has been increased focus on the development of environmentally friendly bio-resources<sup>1–4</sup>. Windmill palm is one of the most cultivated palms in China. Single windmill palm fibers can be extracted from this raw cellulose-material resource. Basic information on the windmill-palm fiber, as well as the single fibers, is shown in Table 1<sup>5</sup>. However, to date, this abundant, inexpensive, and bio-compatible cellulose resource has not been utilized commercially<sup>6,7</sup>. Short, single, windmill-palm fibers, with an average length of about 600 μm, are not suitable for clothing purposes, and are therefore generally discarded as waste<sup>5</sup>. However, a lumen exists in the center of these windmill-palm fibers; this hollow structure can increase the friction that exists between sound waves and the fibers. Therefore, these windmill-palm fibers could potentially be applied to prepare nonwoven fabrics with good acoustic properties<sup>8</sup>. While, high levels of noise pollution can cause various types of public health hazards, such as deafness, and even heart ailments<sup>9</sup>.

The acetylation treatment process is attractive and simple, and is widely applied to modify the hydroxyl (OH) groups on the cellulose surface<sup>10,11</sup>. The key to this method is to replace the OH groups of the fiber with acetyl (CH<sub>3</sub>CO) groups. Many researchers use this treatment to improve the fiber–matrix adhesion of cellulose fiber/polymer composites<sup>8,12</sup>. However, there have been no reports on the use of waste windmill-palm fibers as raw materials for the development of hydrophobic materials, especially with excellent sound-absorption properties.

In this study, alkalinized and acetylated single windmill-palm fibers were prepared and their microstructure, hydrophobic properties, and acoustic properties were investigated. Such acetylation treatments are considered to be a novel method for the preparation of lightweight, nonwoven fabrics with good acoustic performances.

### Results

**Acetylation treatment and hydrophobic properties.** Prior to the orthogonal design, single-factor tests were conducted. At the start of the treatment, the contact angle increases with the acetyl chloride concentration, pyridine concentration, temperature, and time, respectively. Subsequently, the contact angle slightly decreases as the reagent concentration further increases. Consequently, an orthogonal design involving four-factor and three-level experiment was used to optimize the parameters used for the modification of the windmill palm fiber, in which the fiber would develop a hydrophobic surface. The details are shown in Table 2.

<sup>1</sup>College of Textile and Clothing Engineering, Soochow University, Suzhou, 215006, Jiangsu, China. <sup>2</sup>Nantong Textile & Silk Industrial Technology Research Institute, Nantong, 226108, Jiangsu, China. Correspondence and requests for materials should be addressed to G.W. (email: [wanguohe@suda.edu.cn](mailto:wanguohe@suda.edu.cn))

Samples	Chemical composition/%				Physical structure/ $\mu\text{m}$		
	Ash	Lignin	$\alpha$ -Cellulose	Hemi-Cellulose	Length	Diameter	Hollowness /%
Windmill palm fiber	1.23	23.52	52.26	19.23	$3.71 \times 10^5$	400	—
Single fiber	0.54	7.24	78.18	11.32	637.96	10.01	47.21

**Table 1.** The chemical compositions and physical structures of the windmill palm fiber and single fiber.

Level	Factor			
	A acetylchloride/vt.%	B pyridine/vt.%	C Temperature/ $^{\circ}\text{C}$	D Time/h
1	7.5	2.5	30	4
2	12.5	5.0	40	6
3	17.5	7.5	50	8

**Table 2.** Factors and levels of the orthogonal design.

Samples	Factor Result				
	A	B	C	D	Contact angle/ $^{\circ}$
1	1	1	1	1	126.48
2	1	2	2	2	133.28
3	1	3	3	3	136.08
4	2	1	2	3	136.95
5	2	2	3	1	141.25
6	2	3	1	2	142.35
7	3	1	3	2	133.78
8	3	2	1	3	140.58
9	3	3	2	1	139.70
$K_1$	395.83	397.20	409.40	407.43	
$K_2$	420.55	415.10	409.93	409.40	
$K_3$	414.05	418.13	411.10	413.60	
R	24.73	20.93	1.70	6.17	

**Table 3.** The characteristics of the fibers treated under various conditions.

The effects of the four factors on the contact angle of the windmill-palm fiber are shown in Table 3. As shown, factor A (concentration of acetyl chloride), with the highest range (R), has the greatest influence on the contact angle. In addition, the temperature, with the smallest R, only has a slight influence on the hydrophobic properties of the windmill palm fiber. As shown in the Table 3, the parameters with the highest K (the sum of contact angle) values can be considered optimal. In general, the optimal parameters for modification of the natural windmill palm fibers can be considered to be 12.5 vt.% acetyl chloride, 7.5 vt.% pyridine, temperature of 50  $^{\circ}\text{C}$ , and treatment time of 8 h.

Following the treatment under the optimal parameters, the static water-contact angles of the windmill-palm fiber increased from  $20 \pm 6^{\circ}$  to  $143 \pm 4^{\circ}$ . In addition, Fig. 1 shows that the nature of the surface changed from hydrophilic to hydrophobic. The acetylation treatment replaces the OH groups on the cell walls of the windmill palm fibers with  $\text{CH}_3\text{CO}$  groups, which decreases the number of OH groups present on the fiber surface. This causes the hydrophilic windmill palm fibers to transform into hydrophobic fibers.

**Morphological investigation of the alkalinized and acetylated windmill palm fibers.** The ligno-cellulose windmill palm fiber is a natural composite that is primarily composed of cellulose, hemicellulose, and lignin. The cellulose, which has a high degree of crystallinity, has an important function of reinforcement<sup>13</sup>. Owing to hydrolysis, hemicellulose is soluble in alkali, and compared with cellulose, is expected to exhibit poor stability in dilute alkali solutions. This is because the hemicellulose possesses a branched structure while the cellulose has a linear structure<sup>14,15</sup>. Lignin can be solubilized via alkali treatments. This improves the solubility of the lignin in the solution<sup>16</sup>. The alkalization of the windmill palm fibers resulted in the hydrolysis of the composite fiber bundles, forming single fibers. This was due to the solubilization of the hemicellulose and the partial degradation of the lignin. The single fibers consist of hydrophilic cellulose fibers that each possess a large lumen in the center of their cross section<sup>5</sup>. The change in the morphology of the alkalinized, single windmill palm fiber following the acetylation treatment is shown in Fig. 2. Irregularly shaped, aggregated fibrils can be observed in Fig. 2(a). The dense surface wall of the fiber can be clearly observed even when it is by magnified  $\times 90\text{K}$ . Meanwhile, Fig. 2(b) shows that the aggregation has disappeared following the chemical treatment, and large numbers of nanoscale pores have formed. The mean pore size ranges from 10 to 50 nm.

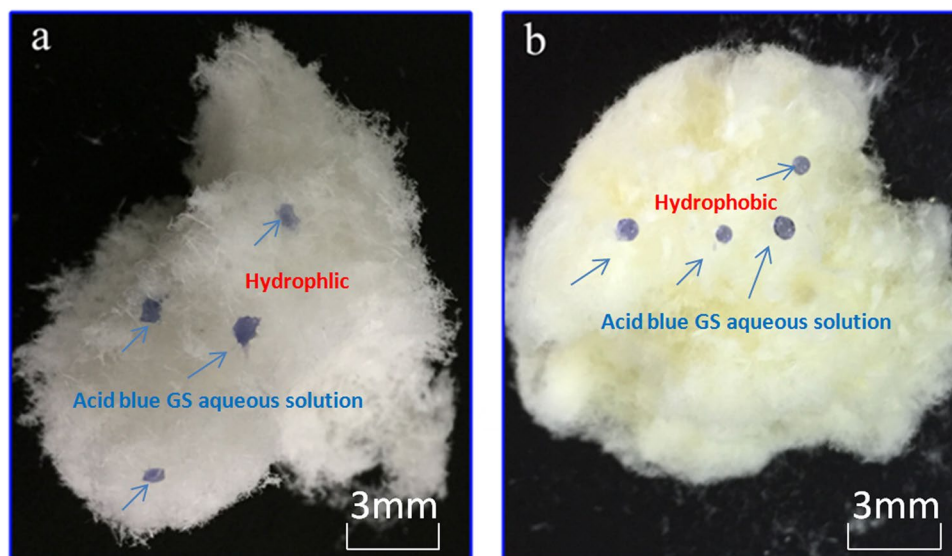


**Figure 1.** Images of (a) alkalinized single windmill palm fiber, and (b) acetylated single fiber.

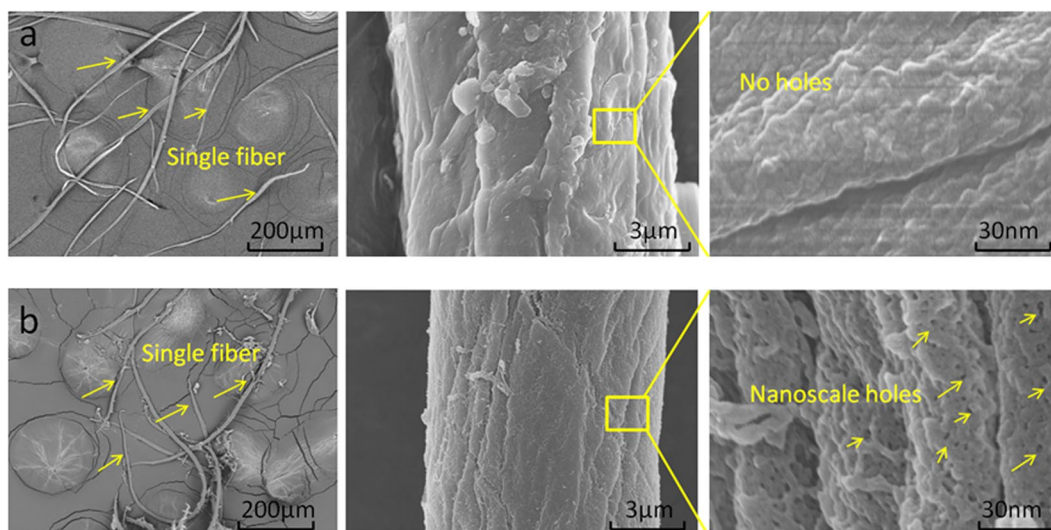


**Figure 2.** Surface morphologies of (a) alkalinized single windmill palm fiber, and (b) acetylated fiber.

**Chemical composition.** The Fourier-transform infrared (FTIR) spectra of the windmill palm fiber, alkalinized single fiber, and acetylated single fiber are shown in Fig. 3. All the windmill-palm fibers exhibited broad absorption peaks at around  $3400\text{ cm}^{-1}$  and  $2900\text{ cm}^{-1}$ , which were attributed to OH stretching and CH stretching, respectively<sup>17</sup>. The lignin presented characteristic peaks over the range of  $1500\text{--}1600\text{ cm}^{-1}$ , which were attributed to the aromatic C=C stretching of the aromatic ring of the lignin<sup>18</sup>. In addition, the windmill palm fiber exhibited a peak at  $1740\text{ cm}^{-1}$ , which corresponded to the C=O stretching of the  $\text{CH}_3\text{CO}$  groups of the hemicelluloses<sup>19</sup>. While, in the cases of the alkalinized and acetylated fibers, these peaks were absent. This indicates that lignin and hemicellulose were not present in these fibers.

The peaks at around  $1400\text{ cm}^{-1}$  can be attributed to the C- $\text{CH}_3$  band<sup>20</sup>. The absorption peaks at  $1640\text{ cm}^{-1}$  can be attributed to the OH stretching of the water absorbed by the cellulose<sup>21</sup>. In the case of the acetylated fiber, the peaks at  $1757\text{ cm}^{-1}$  could be attributed to the C=O stretching of the carbonyl groups of the ester bonds<sup>22</sup>. The vibration peaks at about  $1240\text{ cm}^{-1}$  can be attributed to the C-O stretching of the  $\text{CH}_3\text{CO}$  groups<sup>22</sup>. These two peaks confirmed the acetylation of the windmill palm fiber<sup>22</sup>.

**Absorption properties.** Figure 4 presents the moisture-absorption curves obtained for the windmill palm fiber, and the alkalinized and acetylated single fibers. In the cases of the three samples, the initial rate of moisture absorption is extremely rapid. The curves decrease from 30 to 300 min for the windmill palm fiber. And this decrease for alkalinized fiber and acetylated fiber were from 16 to 80 min, and 10 to 50 min respectively. The raw, alkalinized, and acetylated fibers all achieve moisture sorption equilibrium following a period of 5 h. The alkali

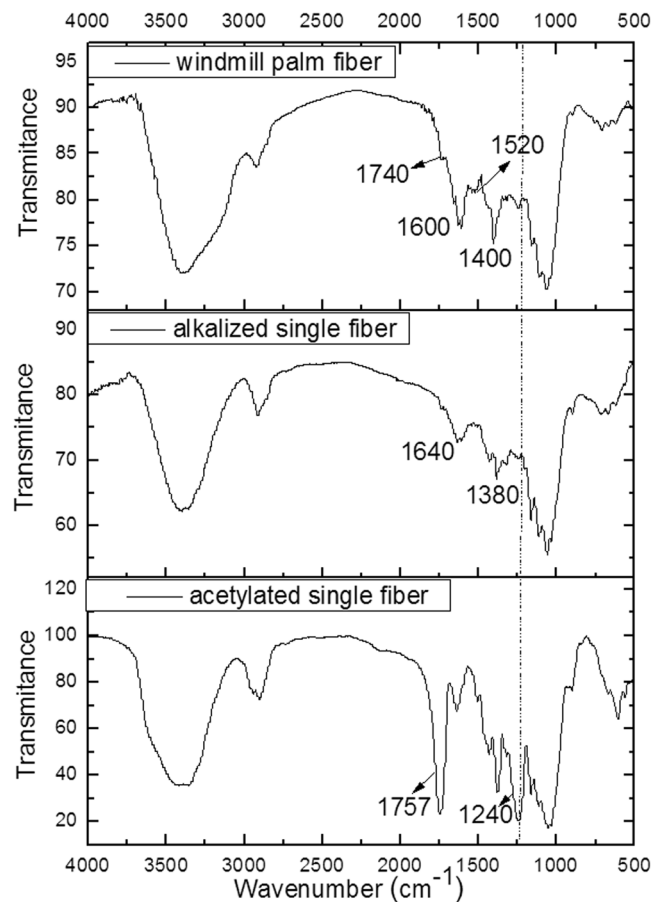


**Figure 3.** FTIR spectra of windmill palm materials.

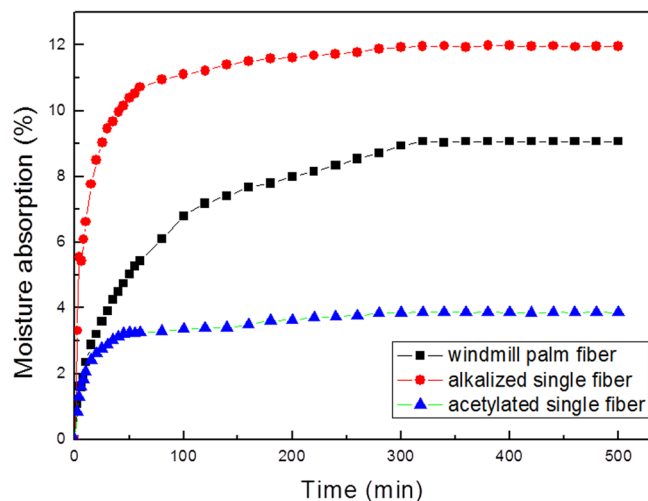


**Figure 4.** The moisture absorption curves obtained for the raw and treated windmill palm fibers.

treatment resulted in the removal of the hydrophobic wax and silica from around the fiber surface. The OH groups of the cellulose react with the water molecules, which contributes to the increased water absorption<sup>23,24</sup>. The swelling of the alkalinized single fiber also contributes to the increase in the moisture absorption<sup>25–27</sup>. Thus, in this study, the moisture regain value of the alkalinized single fiber is the highest, namely 11.96%.

The windmill palm fiber demonstrates a moisture regain value of 9.07%; this is slightly lower than that of the alkalinized single fiber, but greater than those of cotton (7.48%) and flax (8.51%)<sup>7</sup>. As shown in Table 1 and Fig. 2, the palm fiber prepared directly from the sheath mesh exhibits low crystallinity, a rough morphology, an abundance of hollow fiber cells, and a relatively high hemicellulose content. These factors contribute to the excellent moisture

Project	Sum of squares III	$d_f$	Mean square	F	Significance
Correction model	4.561	21	0.217	28.894	0.000
Intercept	6.936	1	6.936	922.696	0.000
Frequency	4.451	19	0.234	31.167	0.000
Sample	0.110	2	0.055	7.300	0.002
Error	0.286	38	0.008		
Sum	11.783	60			
Correction of a total	4.847	59			

**Table 4.** Results of one-way ANOVA test that examined the effects of the surface modification of the windmill-palm fibers on their sound absorption properties.

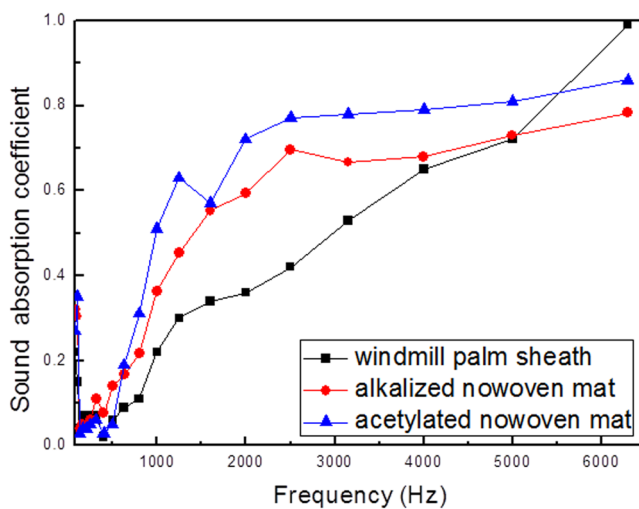


**Figure 5.** Sound absorption coefficients of the various nonwoven windmill palm fabrics.

absorption properties of this fiber. In the case of the acetylated fiber, the moisture regain value is extremely low, namely 3.86%.

**Acoustic properties of the windmill-palm fibers.** Alkalized nonwoven windmill palm fabric, acetylated nonwoven fabric, and raw palm sheath samples, each with a thickness of about 8 mm and diameter of 10 mm, were prepared. The weights of the three material samples were 5 g, 5 g, and 10 g, respectively.

Figure 5 presents the absorption performance of the alkalized windmill palm fiber, acetylated fiber, and palm sheath materials. As shown, amongst the samples tested, the acetylated nonwoven fabric exhibits relatively high levels of absorption. Over the frequency range of 80 to 6300 Hz, the average sound absorption coefficients of the alkalized, nonwoven windmill-palm fabric, acetylated nonwoven fabric, and palm sheath samples were 0.31, 0.36, and 0.23, respectively.

To further verify the effect of the surface modification on the sound absorption properties of the windmill palm fibers, detailed statistical analysis was also performed; the results are shown in Table 4. The results show that prior to, and following the surface modification, there a significant difference in the sound absorption coefficient ( $P \leq 0.05$ ). Thus, we conclude that the alkali treatment, as well as the acetylation treatment, has a significant positive affect (Significance = 0.002) on the acoustic properties of the fibers. The acetylated fiber possesses nanoscale (10 to 50 nm) pores on its surface. Owing to this unique microstructure, the acetylated windmill palm fiber is considered a novel raw material for the preparation of sound-absorbing nonwoven fabrics. The nanoscale pore structure of the materials can significantly increase their specific area and surface permeability. This indicates that sufficient space exists for the transfer of sound. This consequently has a positive effect on acoustic insulation<sup>28,29</sup>. The mass of the acetylated sample is half that of the nonwoven windmill palm fabric sample, and its average sound absorption coefficient is 0.36. This information can be used for the development of novel, acoustic bio-cellulose materials.

## Discussion

The chemical modification results in the substitution of the OH groups of the cell walls of the cellulosic fibers with  $\text{CH}_3\text{CO}$  groups<sup>12</sup>. The reduction in the number of OH groups results in the destruction of the connections among the cellulose components. This results in the development of a rough surface with pores of various sizes. The reduction in the number of OH groups also results in lower moisture absorption, a lower degree of swelling, and reduces the presence of voids at the interface<sup>30</sup>. It also has a positive effect on the stress transfer from the matrix to the fiber<sup>31,32</sup>.

Samples	Acetylchloride/vt.%	Pyridine/vt.%	Temperature/°C	Time/h
1	7.5	2.5	30	4
2	7.5	5.0	40	6
3	7.5	7.5	50	8
4	12.5	2.5	40	8
5	12.5	5.0	50	4
6	12.5	7.5	30	6
7	17.5	2.5	50	6
8	17.5	5.0	30	8
9	17.5	7.5	40	4

**Table 5.** The parameters of the acetylation treatment.

Owing to the acetylation treatment, the surface of the single windmill palm fiber became hydrophobic. Under high-humidity environmental conditions, the hydrophobic surfaces are not wetted by the liquid. Instead, air inclusions or vacuums are formed, which lead to lower energy losses compared with those of hydrophilic surfaces<sup>33</sup>. Owing to the pore structure formed by the random arrangement of fibers, the 47% hollow structure of each single fiber, and the presence of nanoscale pores on the cell walls of the fiber, the porosity level of the material changed from the nanometer to the micrometer scale. In addition, the nanoscale holes formed by the acetylation treatment increased the size of the space available for the transfer of sound and increased the roughness of the fiber-cell wall<sup>29</sup>. Owing to the viscous damping and thermal loss caused by their complicated pore structures, the nonwoven fibrous fabrics demonstrate superior sound absorption capability<sup>34,35</sup>.

## Materials and Methods

**Materials.** The windmill palm sheath meshes were obtained from Mount Huang, Anhui province, China. The windmill palm fibers were treated with a 4 wt.% hydrogen peroxide (H<sub>2</sub>O<sub>2</sub>) and 1.5 wt.% sodium hydroxide (NaOH) solution, with a 1:50 fiber-to-extractant ratio (g/mL), at 85 °C for 4 h<sup>5</sup>. The fiber suspension for was stirred for about 2 min. Subsequently, separate, alkalinized single windmill palm fibers were obtained. These single fibers were filtered and dried in an oven at 60 °C for 24 h.

Subsequently, 1 g of the dried, alkalinized, single windmill-palm fibers was immersed in 20 mL of dimethyl formamide (DMF). This mixture was stirred occasionally for 20 min; subsequently, various amounts of acetyl chloride and various concentrations of pyridine were added. The resultant mixture was held for various periods and temperatures based on the results of the orthogonal design. The parameters of each test are shown in Table 5.

Following the acetylation treatment, the fibers were washed with distilled water, dried at 60 °C, and stored. The alkalinized and acetylated single windmill-palm fibers were obtained. The nonwoven fabric, shown in Fig. 6, was prepared using a wet laying technique<sup>29</sup>.

**Contact-angle measurement.** A contact-angle goniometer (DSA 100 S, KRUSS, Germany) was employed to measure the contact angle of the nonwoven windmill palm fabric. A dosing volume of 3 μL of water was placed onto the surface of each sample, and the contact angle was measured. This procedure was repeated three times.

**Characterization of single windmill-palm fibers.** The surfaces of the alkalinized and acetylated single windmill-palm fibers were observed using scanning electron microscopy (SEM; S-4800, HITACHI, Japan). The samples were gold sputtered for 20 s. An accelerating voltage of 5 kV was used, along with a working distance of 8.9 mm.

**Moisture regain test.** The moisture regain values of the windmill palm fibers and single fibers were determined using the method described in standard GB/T 9995-1977. About 1.0 g of the fiber samples was dried at 105 °C in a hot-air oven for 4 h. The weight of the dried fiber was denoted as *W<sub>a</sub>*. The fibers were then allowed to regain moisture under a standard atmosphere of 65% RH and 20 °C. Initially, the weight of the fibers was recorded every 5 min, and subsequently, every 20 min until the fibers achieved moisture sorption equilibrium. The weight of each of the samples, at a specific time, was recorded as *W<sub>i</sub>*. The moisture regain value was determined by the following equation (Eq. (1)):

$$\text{Moisture regain(\%)} = (W_a - W_i)/W_a * 100 \quad (1)$$

**Sound absorption measurement.** The normal incidence absorption coefficient was determined using two microphone impedance tubes (SW463, Shengwang, China). This was achieved by employing the transfer function method over the frequency range of 80 Hz to 6300 kHz. The average sound absorption coefficient was calculated by determining the mean of the absorption coefficients at 125, 250, 500, 1000, 2000, and 4000 Hz.

## Conclusions

In summary, hydrophobic windmill-palm fibers, with a moisture regain value of 3.86% and contact angle of about 143 ± 4°, were prepared by performing an acetylation treatment at 50 °C for 8 h, with 12.5 vt.% acetyl chloride and 7.5 vt.% pyridine. The acetylated fiber possessed nanoscale (from 10 to 50 nm) pores on its surface. Owing to its unique microstructure, the acetylated windmill-palm fiber can be considered a novel raw material for the

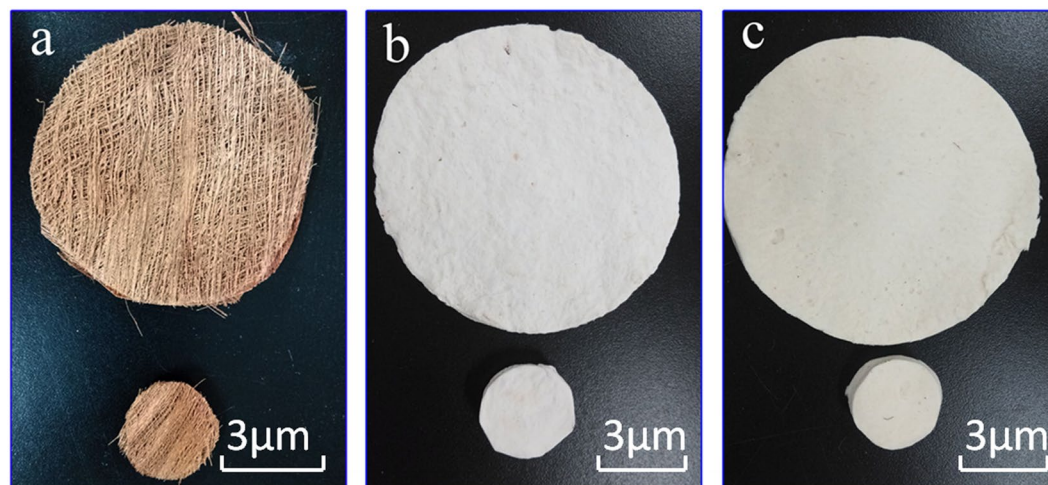


**Figure 6.** Samples of (a) windmill palm mesh, (b) alkalinized, nonwoven single fiber fabric, and (c) acetylated nonwoven fabric.

preparation of sound-absorbing nonwoven fabrics. The weight of the acetylated fabric is half that of the nonwoven windmill palm fabric, and its average sound absorption coefficient is 0.36, which is even higher than that of the nonwoven windmill palm fabric (0.31). The results of this study can be used for the development of novel, acoustic bio-cellulose materials.

## References

- Xu, Y., Li, Y., Zhang, A. & Bao, J. Epoxy foams with tunable acoustic absorption behavior. *Mater. Lett.* **194**, 234–237 (2017).
- Koruk, H. & Genc, G. Investigation of the acoustic properties of bio luffa fiber and composite materials. *Mater.Lett.* **157**, 166–168 (2015).
- Reddy, N. & Yang, Y. Properties of high-quality long natural cellulose fibers from rice straw. *J. Agr. food Chem.* **54**, 8077–81 (2006).
- Reddy, N. & Yang, Y. Structure and properties of natural cellulose fibers obtained from sorghum leaves and stems. *J. Agr. food Chem.* **55**, 5569–74 (2007).
- Chen, C., Sun, G., Chen, G., Li, X. & Wang, G. Microscopic structural features and properties of single fibers from different morphological parts of the windmill palm. *BioResources* **12**, 3504–3520 (2017).
- Zhai, S., Li, D., Pan, B., Sugiyama, J. & Itoh, T. Tensile strength of windmill palm (*Trachycarpus fortunei*) fiber bundles and its structural implications. *J. Mater. Sci.* **47**, 949–959 (2012).
- Zhang, T., Guo, M., Cheng, L. & Li, X. Investigations on the structure and properties of palm leaf sheath fiber. *Cellulose* **22**, 1039–1051 (2015).
- Zheng, Y., Wang, J., Zhu, Y. & Wang, A. Research and application of kapok fiber as an absorbing material: A mini review. *J. Environ. SCI.* **27**, 21–32 (2015).
- Ahmed, T. & Rahman, T. Non-Auditory health hazard vulnerability to noise pollution: assessing public awareness gap. *American Journal of Engineering Research* **4**, 143–147 (2015).
- Miao, J., Yu, Y., Jiang, Z. & Zhang, L. One-pot preparation of hydrophobic cellulose nanocrystals in an ionic liquid. *Cellulose* **23**, 1209–1219 (2016).
- Maim, C. J., Mench, J. W., Kendall, D. L. & Hiatt, G. D. Aliphatic acid esters of cellulose. Preparation by acid-chloride-pyridine procedure. *Ind. Eng. Chem. Res.* **43**, 684–688 (1951).
- Haque, M. M. U., Maniruzzaman, M. & Reza, M. S. Thermal and tensile mechanical behavior of polystyrene graft acetic anhydride-treated pulque fibers. *J. Nat. Fibers.* **13**, 125–136 (2016).
- Arfaoui, M. A., Dolez, P. I., Dubé, M. & David, E. Development and characterization of a hydrophobic treatment for jute fibres based on zinc oxide nanoparticles and a fatty acid. *Appl. Surf. Sci.* **397**, 19–29 (2017).
- Yu, C. H., Feng, X. X., Jia, C. L. & Chen, J. Y. Hemp retting by the combined action of high temperature boiling and enzymes. *Text. Res. J.* **28**, 79–82 (2007).
- Bjerre, A. B., Olesen, A. B., Fernqvist, T., Plöger, A. & Schmidt, A. S. Pretreatment of wheat straw using combined wet oxidation and alkaline hydrolysis resulting in convertible cellulose and hemicellulose. *Biotechnol. Bioeng.* **49**, 568–577 (1996).
- Hartley, R. D. Degradation of cell walls of forages by sequential treatment with sodium hydroxide and a commercial cellulase preparation. *J. SCI. Food Agric.* **34**, 29–36 (1983).
- Tian, M. *et al.* Enhanced mechanical and thermal properties of regenerated cellulose/graphene composite fibers. *Carbohydr. Polym.* **111**, 456–462 (2014).
- Morán, J. I., Alvarez, V. A., Cyras, V. P. & Vázquez, A. Extraction of cellulose and preparation of nanocellulose from sisal fibers. *Cellulose* **15**, 149–159 (2008).
- Rout, A. K., Kar, J., Jesti, D. K. & Sutar, A. K. Effect of Surface Treatment on the Physical, Chemical, and Mechanical Properties of Palm Tree Leaf Stalk Fibers. *BioResources* **11**, 4432–4445 (2016).
- Kim, D. Y., Nishiyama, Y. & Kuga, S. Surface acetylation of bacterial cellulose. *Cellulose* **9**, 361–367 (2002).
- Li, R. *et al.* Cellulose whiskers extracted from mulberry: A novel biomass production. *Carbohydr. Polym.* **76**, 94–99 (2009).
- Jonoobi, M., Harun, J., Mathew, A. P., Hussein, M. Z. B. & Oksman, K. Preparation of cellulose nanofibers with hydrophobic surface characteristics. *Cellulose* **17**, 299–307 (2010).
- Sarifuddin, N., Ismail, H. & Ahmad, Z. The effect of kenaf core fibre loading on properties of low density polyethylene/thermoplastic sago starch/kenaf core fiber composites. *J. Phys. Sci.* **24**, 97–115 (2013).
- Datta, J. & Kopczyrska, P. Effect of kenaf fibre modification on morphology and mechanical properties of thermoplastic polyurethane materials. *Ind. Crop. Prod.* **74**, 566–576 (2015).

25. Abraham, E. *et al.* R. Extraction of nanocellulose fib-rils from lignocellulosic fibres: a novel approach. *Carbohydr Polym.* **86**, 1468–1475, <https://doi.org/10.1016/j.carbpol.2011.06.034> (2011).
26. Tan, B. K., Ching, Y. C., Gan, S. N., Ramesh, S. & Rahmmah, R. V. Water absorption properties of kenaf fibre—PVA composites. *Mater. Res. Innov.* **18**, 144–146 (2014).
27. Goh, K. Y., Ching, Y. C., Chuah, C. H., Abdullah, L. C. & Liou, N. S. Individualization of microfibrillated celluloses from oil palm empty fruit bunch: Comparative studies between acid hydrolysis and ammonium persulfate oxidation. *Cellulose* **23**, 379–390 (2016).
28. Pu, H., Wang, D. & Yang, Z. Towards high water retention of proton exchange membranes at elevated temperature via hollow nanospheres. *J. Membrane Sci.* **360**, 123–129 (2010).
29. Yao, R., Yao, Z. & Zhou, J. Pore morphology and acoustic properties of open-pore phenolic cryogel acoustic multi-structured plates. *Mater. Lett.* **176**, 199–201 (2016).
30. Ashori, A. Wood-plastic composites as promising green-composites for automotive industries. *Bioresource Techn.* **99**, 4661–4667 (2008).
31. Venkateshappa, S. C., Jayadevappa, S. Y. & Puttiah, P. K. W. Mechanical behavior of areca fiber reinforced epoxy composites. *Adv. Polym. Tech.* **31**, 319–330, <https://doi.org/10.1002/adv.20255> (2012).
32. Punyamurthy, R., Sampathkumar, D., Srinivasa, C. V. & Bennehalli, B. Effect of alkali treatment on water absorption of single cellulosic abaca fiber. *BioResources* **7**, 3515–3524 (2012).
33. Ferreira, G. N., Da-Silva, A. C. & Tomé, B. Acoustic wave biosensors: physical models and biological applications of quartz crystal microbalance. *Trends Biotechnol.* **27**, 689–697 (2009).
34. Chen, C., Zhang, Y., Sun, G., Wang, J. & Wang, G. Windmill palm fiber/polyvinyl alcohol coated nonwoven mats with sound absorption characteristics. *BioResources* **11**, 4212–4225 (2016).
35. Chen, W. *et al.* Modeling of sound absorption based on the fractal microstructures of porous fibrous metals. *Mater. Des.* **105**, 386–397 (2016).

## Acknowledgements

This work was funded by the Priority Academic Program Development of Jiangsu Higher Education Institutions, China (No.37 [2014]).

## Author Contributions

Changjie Chen and Guohe Wang conceived and designed the experiments; Changjie Chen, Zhong Wang, and Kaiwei Nie analyzed the data; Changjie Chen, Ming Bi, and You Zhang performed the experiments and Changjie Chen wrote the paper.

## Additional Information

**Competing Interests:** The authors declare no competing interests.

**Publisher's note:** Springer Nature remains neutral with regard to jurisdictional claims in published maps and institutional affiliations.



**Open Access** This article is licensed under a Creative Commons Attribution 4.0 International License, which permits use, sharing, adaptation, distribution and reproduction in any medium or format, as long as you give appropriate credit to the original author(s) and the source, provide a link to the Creative Commons license, and indicate if changes were made. The images or other third party material in this article are included in the article's Creative Commons license, unless indicated otherwise in a credit line to the material. If material is not included in the article's Creative Commons license and your intended use is not permitted by statutory regulation or exceeds the permitted use, you will need to obtain permission directly from the copyright holder. To view a copy of this license, visit <http://creativecommons.org/licenses/by/4.0/>.

© The Author(s) 2018